

Measuring packing length in simulations for different polymer architectures

Sai Vineeth Bobbili and Scott T. Milner^{a)}

Department of Chemical Engineering, The Pennsylvania State University, University Park, Pennsylvania 16802

(Received 26 May 2021; final revision received 9 August 2021; published 14 September 2021)

Abstract

The packing length p figures prominently in scaling predictions of the entanglement length and bulk modulus for polymer melts and solutions. p has been argued to scale as the ratio of chain displaced volume V and mean square end-to-end distance R^2 . This scaling works for several cases; however, it is not obvious how to apply it to chains with side groups, and the scaling must fail for sufficiently thin, stiff chains. In this work, we measure the packing length in simulations, without making any scaling assumptions, as the typical distance of closest approach of two polymer strands in a simulated bead-spring melt. We use the intermolecular correlation function to measure the distance up to which a given polymer strand dominates the local volume fraction. Using our measured packing length, we find good agreement of entanglement properties with Lin–Noolandi scaling for flexible polymers of different architectures. © 2021 The Society of Rheology. https://doi.org/10.1122/8.0000305

I. INTRODUCTION

Entanglements govern the viscoelastic properties of long polymer liquids [1]. Entangled chains are represented as kinetically confined to a tube, arising from uncrossability constraints imposed by neighboring chains [2–4]. The extent of polymer entanglement depends on molecular details of the repeat units. Different entanglement regimes are expected, depending on whether polymer chains are flexible or stiff within the tube. In our view, polymer melts and solutions are as entangled as they can be, limited only by how closely different polymer strands can approach each other, and how readily such strands can change direction to wrap around each other [5].

We are thus interested in the typical distance of the closest approach of two backbone moieties on different strands, which we call the packing length p. This intuitive, qualitative concept has been previously translated to a specific, quantitative definition intended for flexible chains by means of a scaling argument, which we now briefly reprise [6].

Consider a flexible chain segment on a long chain in a polymer melt of identical chains. A segment of mass M, density ρ , and mean-square end-to-end distance R displaces a volume V given by M/ρ and pervades a volume scaling as R^3 . For long segments, the pervaded volume R^3 is much larger than V, with plenty of room for other chain segments. But for a sufficiently short segment, these volumes are comparable, and other chain segments cannot enter the pervaded volume, without overfilling space.

The ratio R^3/V becomes of order unity at some length scale R = p, which implies

$$p \sim \frac{V}{R^2}.\tag{1}$$

For a flexible polymer chain in a melt, the ratio V/R^2 is a material parameter, since both quantities are proportional to the chain length. Hence, for a given polymer architecture, p is a characteristic length over which monomers of a given chain dominate the local density. p thereby governs the typical distance of closest approach of monomers on different chain segments.

This scaling argument for the packing length gives a formula computable from data $[p = M/(\rho R^2)]$. As with any scaling result, the formula omits an unknown coefficient of order unity. Figure 1 shows an interpretation of p, with chain configurations represented as random walks of "packing blobs," which tend not to overlap.

The packing length evidently depends on the chain architecture. Flexible chains have larger p than stiff chains; likewise, bulky chains have larger p than thin chains. Flexible or bulky chains have a stronger tendency to fill up the space around their own monomers. Since the packing length depends on identifiable polymer characteristics, materials can be designed with controllable viscoelastic properties [7,8].

The scaling formula for p can be related to the Kuhn length by defining an average diameter d of the chain such that the displaced volume of a Kuhn segment is $V_K = \pi (d/2)^2 L_K$ (we persist in omitting all factors of order unity). The chain volume V can then be written $V = V_K(L/L_K)$, where L is the chain arc length and L_K is the Kuhn length. Likewise, the mean-square end-to-end distance can be written $R^2 = LL_K$. Combining these, the ratio V/R^2 scales as d^2/L_K , which gives another computable scaling expression for p, namely,

$$p \sim \frac{d^2}{L_K}. (2)$$

The scaling expression Eq. (2) should have a coefficient substantially larger than unity; otherwise, since L_K is typically somewhat larger than d, we would immediately predict

a) Author to whom correspondence should be addressed; electronic mail: stm9@psu.edu

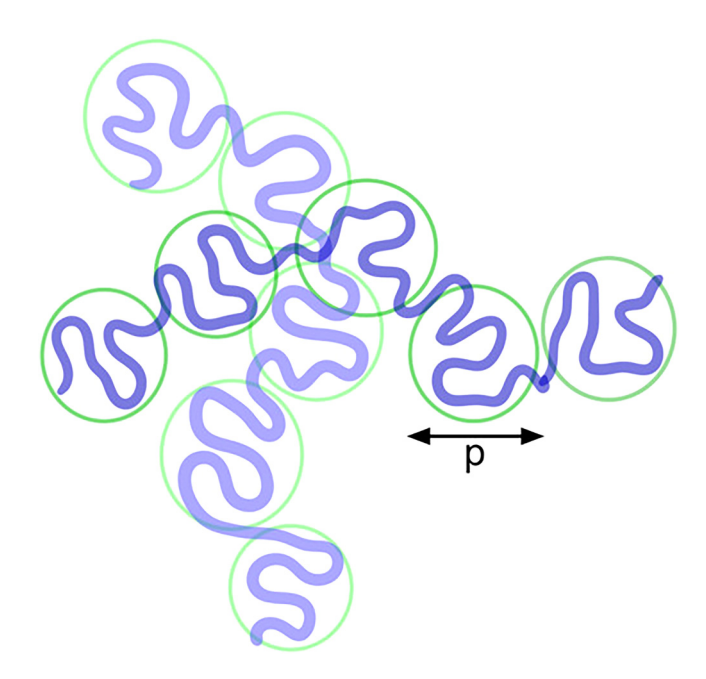


FIG. 1. The packing length dictates the typical distance of separation between polymers. A flexible chain in a melt may be regarded as a random walk of packing blobs. Reprinted with permission from Milner, Macromolecules 53, 1314–1325 (2020). Copyright 2020, American Chemical Society.

p smaller than d, which does not make physical sense. In any case, this scaling predicts that stiffening a chain without increasing its average diameter makes p smaller. Eventually, whatever the prefactor, this scaling result will predict p to be smaller than d.

But if chains are sufficiently stiff, close approaches with other segments should be governed by the chain diameter itself. Since the packing length is defined conceptually as the typical distance of close approaches with other entangling strands, we conclude the scaling result $p \sim V/R^2$ (or equivalently $p \sim d^2/L_K$) must fail for sufficiently stiff chains. Indeed, the scaling argument began with the assumption of chains flexible and bulky enough to fill the space near a given monomer on a strand with other near-neighbor monomers along the same strand. This assumption certainly fails for sufficiently stiff chains.

A complete formula for the packing length, or an algorithm for determining p from simulation trajectories, must crossover from the scaling result d^2/L_K for flexible chains to some measure of the chain diameter for sufficiently stiff chains. However, the length-averaged chain diameter d defined by $V = \pi (d/2)^2 L$ may not always be an appropriate estimate of the packing length for chains in this regime.

The above estimate for d implicitly assumes the chain is a uniform flexible path with a constant diameter. Whereas chains with long flexible side groups attached at intervals along the backbone may have large displaced volumes per unit length, while permitting close contacts with other backbone moieties. In other words, the effective repulsive potential between backbones, mediated by interactions between side groups, may look rather different from a hard-core repulsion with a range set by the length-averaged diameter.

Hence, for flexible and stiff chains alike, scaling estimates for the packing length may be inaccurate or invalid. This is problematic because the packing length plays a central role in modern theories of polymer entanglement, as we shall summarize below. Tests of scaling relations for measured quantities such as the entanglement length N_e , tube diameter a, or plateau modulus G, may fail simply because an invalid estimate of p is employed in the comparison.

In our recent work, we emphasize that comparing the packing length to the Kuhn length determines what entangles, and thus, how often entanglements occur. In the "flexible regime," the packing length is larger than the Kuhn length, and entanglements are close binary encounters of two "packing blobs." When the Kuhn length becomes larger than the packing length, we crossover into the "semiflexible regime," in which entanglements are close encounters of two Kuhn segments.

In the flexible regime, described by the Lin–Noolandi scaling argument, the packing length controls the size of close approaches, and two chain strands can wrap around each other on the same scale. This leads to a scaling prediction for the tube diameter a, namely, $a \sim p$ [9,10]. The LN argument implicitly assumes that chains are flexible in their tubes, so the tube diameter a is larger than the Kuhn length L_K .

The entanglement molecular weight can be obtained from the fact that the entanglement strand consists of a few packing blobs, which are locally meltlike, leading to

$$N_e\Omega_0\sim p^3,$$
 (3)

where Ω_0 is the monomer volume. Correspondingly, the plateau modulus for the melt from the usual assumption of rubber elasticity theory scales as kT per entanglement strand, which gives

$$G \sim kT/p^3$$
. (4)

The LN scaling results are consistent with data compiled by Fetters *et al.* [11] for plateau modulus and packing length of a wide range of polymers. To determine the packing length, chain dimensions were determined by small angle neutron scattering, with results reported as the ratio of mean square end-to-end distance R^2 to molecular weight M. Together with the density $\rho = M/V$, the packing length can be estimated from the scaling relation $p \sim V/R^2$ as $p = M/(\rho R^2)$.

For semiflexible chains, close approaches between chain segments are still governed by the packing length (by definition), which we now expect to be of order the chain diameter. However, entanglement requires segments to change direction, which only happens on the scale of a Kuhn length [5,12]. In this semiflexible regime, entanglement is best described in terms of the arc length density. The arc length density can be written for both melts and solutions in terms of the polymer volume fraction ϕ , and the chain length L and displaced volume V, as $\phi L/V = \phi/d^2$. Note that the ratio L/V is a material parameter (since both L and V are

proportional to chain mass) which scales as $1/d^2$, where d is the length-averaged diameter defined previously.

For solutions and melts of semiflexible chains, entanglement only depends on the arc length density of uncrossable backbone threads, and not on the precise value of their diameter. That is, ϕ and d only appear in the theory in the combination ϕ/d^2 . Then the only remaining length scale is L_K , which determines the size of the binary encounters. Hence, G must scale as $kT(\phi/d^2)^2L_K$ by dimensional analysis, assuming entanglements are binary so the concentration dependence is quadratic.

This result for G can likewise be written in terms of the concentration of Kuhn segments $c = \phi/(\pi(d/2)^2 L_K)$, as $G \sim kTc^2 L_K^3$. This can be interpreted as the probability cL_K^3 that one Kuhn segment encounters another within its pervaded volume, times the concentration of Kuhn segments c, times kT per entanglement.

To summarize: the flexible scaling result for the packing length $p \sim V/R^2$ is limited in its applicability; the precise location of the crossover to the semiflexible regime is a priori unknown; and the length-averaged chain diameter d is problematic as an estimate for p in the semiflexible regime. For these reasons, we are motivated to measure the packing length directly, without employing any scaling estimates, by observations in simulated polymer melts and solutions, of how often backbone moieties on different strands come close to each other. With measured values for p, we can evaluate entanglement scaling relations without being concerned that our estimates of p are in error.

In this work, we obtain the packing length from the radial distribution function $g_{other}(r)$ of neighboring chains near a bead on a reference chain. We integrate $g_{other}(r)$ to obtain in a sphere of radius r the volume fraction of reference chain, and of everything else. We use these volume fractions as functions of r to find the distance at which monomers from other chains start to dominate the density around a given monomer on the reference chain. This approach provides a direct measure of the packing length.

We obtain $g_{other}(r)$ from molecular dynamics simulations of melts of long entangled polymer rings. In our previous work, we developed a chain crossing technique to topologically equilibrate ring polymers [13]. This approach results in a permanently entangled network of ring polymers, which can be regarded as a proxy for infinitely long linear chains, and avoids chain end effects on entanglement properties. To quantify entanglements, we obtain entanglement length N_e through chain shrinking and entanglement modulus G from shearing simulations.

With this approach, we perform a new set of simulations to explore the flexible chain entanglement regime, where LN scaling is expected to apply. We independently control chain bulkiness (by the length of side groups) and stiffness (with backbone angular springs) to move back and forth in the expected degree of entanglement. In this way, we can test whether our new way of measuring p leads to the expected LN scaling for measured properties of the entanglement network.

II. METHODS

In our simulated polymer melts, we use bead-spring polymers with purely repulsive interactions. The beads interact

via the truncated Lennard-Jones potential [Eq. (5)] with cutoff distance $r_c = 2^{1/6}\sigma$. Although not representing any particular polymer, we preserve "atomistic" length and energy scales in our model by choosing σ to be 0.2 nm and ε to be 2.49 kJ/mol (1 kT at 300 K),

$$U_{LJ}(r) = \begin{cases} 4\varepsilon ((\frac{\sigma}{r})^{12} - (\frac{\sigma}{r})^{6}) + \varepsilon, & r \le r_{c}, \\ 0, & r \ge r_{c}. \end{cases}$$
 (5)

We represent the potential between bonded beads with a stiff harmonic spring, given by

$$U_{bond}(r) = (1/2)k_b(r - r_0)^2,$$
 (6)

where $r_0 = 2^{1/6}\sigma$. We use a spring constant k_b equal to $10\,000\,\mathrm{kT/nm^{-2}}$ ($400\,\mathrm{kT/\sigma^2}$).

We study various architectures of polymer chains. The packing length can be varied in two ways: we can increase packing length by making the chains bulky, i.e., by adding side chains, and we can lower the packing length by stiffening the polymer backbone. We also combine both approaches for more control of p.

We increase the backbone stiffness by adding an angular potential of the form $U_a=(1/2)\kappa\theta^2$, with the preferred deflection angle $\theta=0$ corresponding to straight chains. We use bending stiffness values of $\beta\kappa=0$, 0.5, 1, and 2, where $\beta=1/kT$.

To increase the bulkiness of polymer chains, we add short side groups to our linear bead-spring polymers (see Fig. 2). We explore up to three side chain beads per backbone bead (noted in Figs. 5–8 as "sc"). The addition of side groups increases the packing length, making the polymers less entangled.

Combining these two variations in polymer chain architecture, we have a set of 12 different systems for which increases in the side chain length should decrease entanglement, and increases in chain stiffness should increase entanglement. Previously, we varied the chain stiffness of polymers with no side groups to explore the semiflexible and stiff regimes [13]. In this work, we simulated new systems where we vary the backbone stiffness of polymers with small

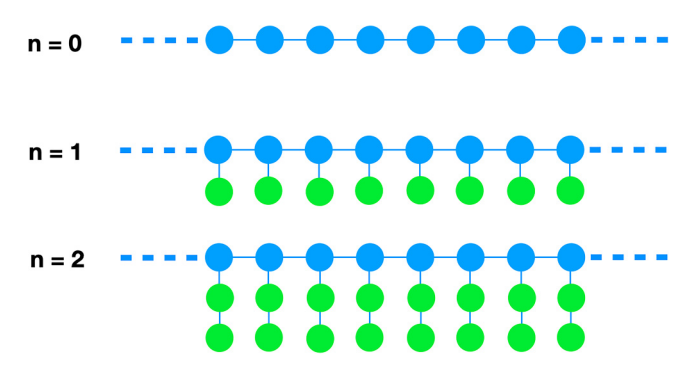


FIG. 2. Ring polymers with sc = 0, 1, and 2 side group beads per backbone bead. Polymer chains are made bulkier by adding side groups. Side chain beads (green; away from the dashed line) have similar properties as backbone beads (blue; along the dashed line), except that we only consider backbone beads when measuring the radial distribution function $g_{other}(r)$.

side chains attached. Based on our previous work, we expect all these new systems to be in the flexible entanglement regime, for which LN scaling should hold.

Our melts consist of 40 rings of 800–1600 repeat units each. We use longer polymers when side groups are involved to ensure an adequate number of entangled strands in the polymer chain, since making the chains bulkier makes them less entangled. We generate initial chain configurations by constructing a random walk of N steps, computing its end-to-end vector R, and adding -R/N to all N bond vectors so that the ring closes. The number density of beads to represent a melt is taken as $0.7/\sigma^3$.

Ring polymers offer several advantages over linear chains in entanglement simulations [14]. A system of long entangled rings in periodic boundary conditions can be regarded as a proxy for a system of infinitely long chains. Entanglements in a topologically equilibrated melt of rings are permanent.

A simulated melt of polymer rings can be equilibrated by allowing the chains to cross each other. This allows access to different topological states and relieves the entanglement constraint. In our previous work [13], we introduced a technique that allows chains to cross by weakening the repulsion between the beads. To control the crossing frequency of the chains, we vary the overall strength of the interaction with a multiplying factor f. For a sufficiently small f, chains cross readily; as f increases toward unity, chain crossing ceases. We smoothly round off the repulsive Lennard-Jones interactions to a parabolic dependence below a short-distance cutoff to avoid problems associated with a singular repulsive potential. We start the simulation with f=0 and slowly raise the value of f toward unity to obtain an equilibrated melt configuration with appropriate interactions as described by Eq. (5).

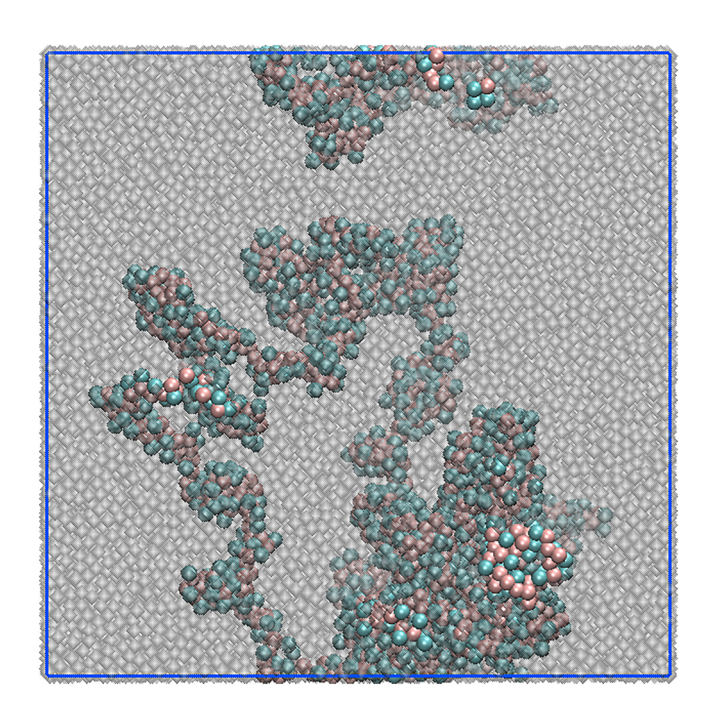


FIG. 3. Simulation snapshot shows the front view of a periodic simulation box that differentiates a reference chain from its neighbors. Pink beads are backbone, blue beads are side groups, and gray (glassy) beads are from surrounding chains.

Once we have an equilibrated melt of long entangled rings, we use chain-shrinking technique to obtain a network of primitive paths and measure the entanglement length N_e . Our algorithm to obtain primitive path network is a combination of the technique originally proposed by Everaers *et al.* [15,16] and the Z1 code by Kroger [17,18]. To directly measure entanglement modulus, we induce shear by deforming the simulation box. A detailed description of both equilibration and analysis techniques can be found in our previous publication [13].

We use the radial distribution function $g_{other}(r)$ of neighboring chains near a bead on a reference chain to obtain packing length. $g_{other}(r)$ describes how the density of beads on other chains varies as a function of distance from a reference bead (see Figs. 3 and 4). With $g_{other}(r)$, we can find out at a given distance from a reference chain, if it is more likely to find a monomer from the chain itself or from other chains. For chains with side groups, we measure $g_{other}(r)$ only for backbone beads, since the short side groups do not entangle.

III. RESULTS AND DISCUSSION

The radial distribution function $g_{other}(r)$ depends on chain architecture. As we stiffen the chains, it is more likely to find monomers from other chains near a reference chain. This is evident in Fig. 5(a), where we see a higher value of $g_{other}(r)$ for the stiffest chain (purple curve) at smaller distances. All the curves evidently approach unity at large r; but, how quickly these curves increase to a point at which monomers from other chains dominate, depends on stiffness in a controlled way.

Similarly, $g_{other}(r)$ depends on the bulkiness of a chain. As we make chains bulky by adding small side groups, it is less likely to find monomers from other chains near a chosen reference chain. This is shown in Fig. 5(b), where $g_{other}(r)$ for bulkier chains is lower at small distances.

We calculate radial volume fraction $F_{other}(r)$ by integrating $g_{other}(r)$ over a spherical volume [see Eq. (7)]. $F_{other}(r)$ is the volume fraction of monomers from chains other than the reference chain within a distance r from the reference chain. This function at large distances will be (N-1)/N, where N is the number of chains in the system. This value is close to

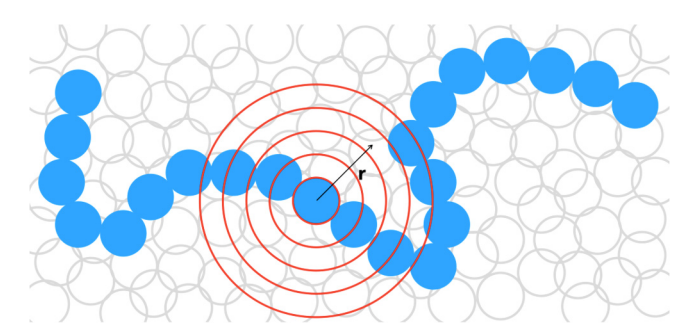


FIG. 4. Radial distribution function can be used to measure the fraction of volume occupied by surrounding chains up to a certain distance. Such volume fraction is obtained using Eq. (7).

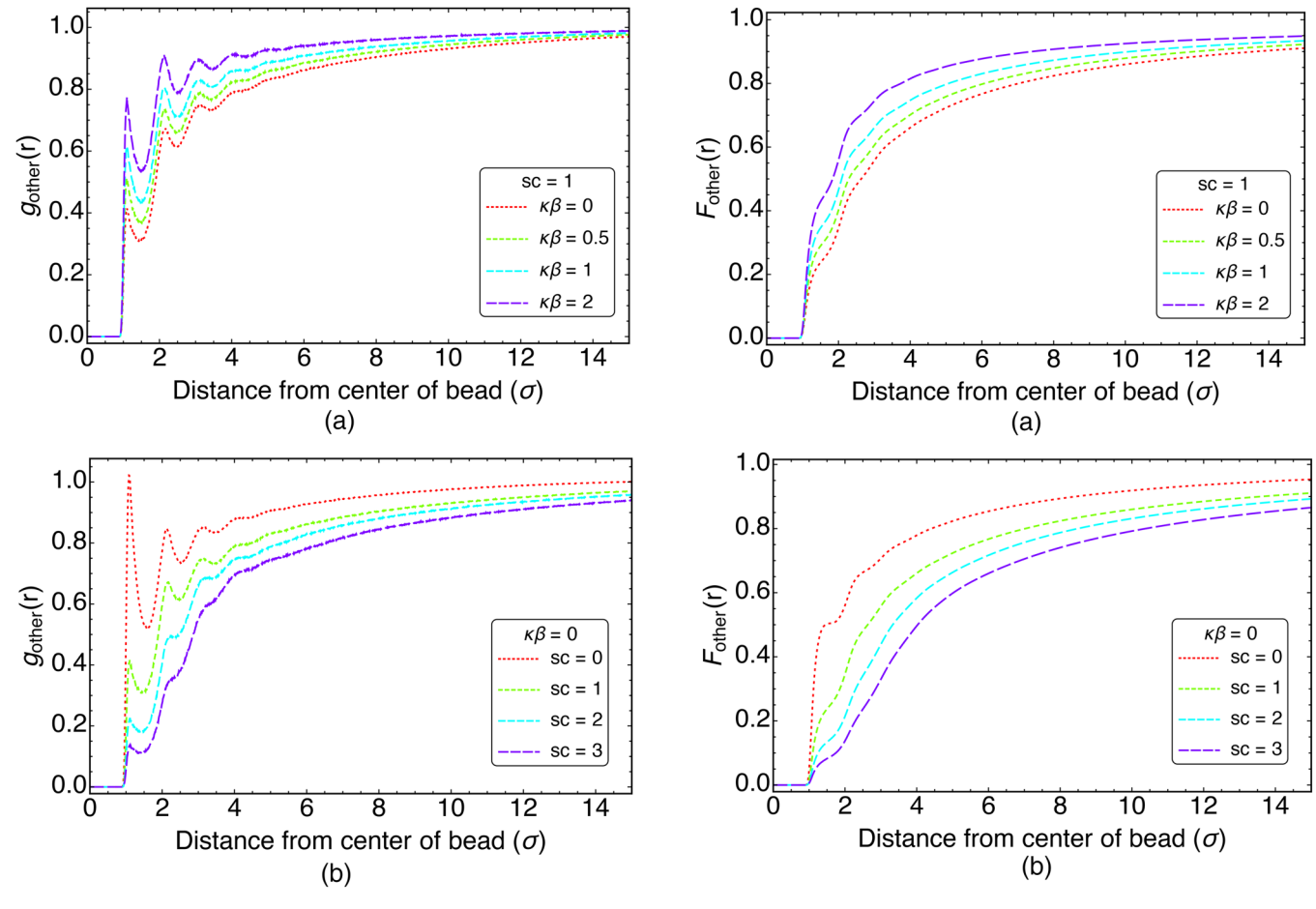


FIG. 5. Radial distribution function of "other" chains. (a) Stiffening the chains results in a higher $g_{other}(r)$ and (b) adding bulky side groups leads to smaller $g_{other}(r)$ at smaller distances.

FIG. 6. Radial volume fraction of "other" chains. (a) Stiffening the chains results in a higher fraction and (b) adding bulky side groups leads to a smaller fraction of "other" chains near a reference chain of interest.

unity as most of the monomers come from other chains,

$$F(r) = \frac{\int_0^r g(r') 4\pi r'^2 dr'}{\frac{4}{3}\pi r^3} * \frac{N-1}{N}.$$
 (7)

Reflecting the behavior of the radial distribution function, stiffer chains have a higher volume fraction $F_{other}(r)$ of monomers from other chains at small values of r. Bulky chains have more monomers from the same chain near a given monomer. This leads to a lower volume fraction $F_{other}(r)$ of monomers from other chains at smaller distances r. At long distances, all chains will have the same $F_{other}(r)$ equal to a saturation value of (N-1)/N, but the rate at which this value is approached depends on the architecture. This behavior is observed in Fig. 6, where flexible and bulky chains have more nearby monomers coming from their own chain.

We use the radial volume fractions to identify the exact distance up to which monomers predominantly come from the same chain. We define the packing length as the distance at which the radial volume fraction $F_{other}(r)$ equals 0.5. At this characteristic distance, monomers from neighboring chains start to dominate the local density.

The packing length defined in this way can never be less than the chain diameter. As evident in Figs. 7 and 8, we often obtain a value of p less than the chain diameter when using the expression V/R^2 . Such a value for p is not realistic. Using $g_{other}(r)$ to measure p always gives a value greater than or equal to d.

The packing length measured using $g_{other}(r)$ restores LN scaling [Eqs. (3) and (4)]. Figures 7 and 8 show good agreement for both N_e and modulus with LN scaling when p is measured using radial distribution function. According to Eq. (3), data in Fig. 7 should collapse on to a slope of 3, which happens in Fig. 7(b) but not in Fig. 7(a). Similarly, Eq. (4) suggests that the data in Fig. 8 should collapse to a slope of -3. This collapse is observed in Fig. 8(b) but not in Fig. 8(a). This suggests that measuring p using $g_{other}(r)$ is more reliable than using Eq. (1), which can give erroneous values for certain chain architectures.

For sufficiently stiff chains, packing length, by definition, is equal to the chain diameter d. In Fig. 9, we compare p measured using F_{other} and as V/R^2 for semiflexible and stiff polymers without any side chains. We expect such chains to be outside the flexible regime and hence, not following the LN scaling. p measured using F_{other} is almost equal to d for the stiff polymers, as should be the case. Only at low values of stiffness, where we are about to enter the flexible regime,

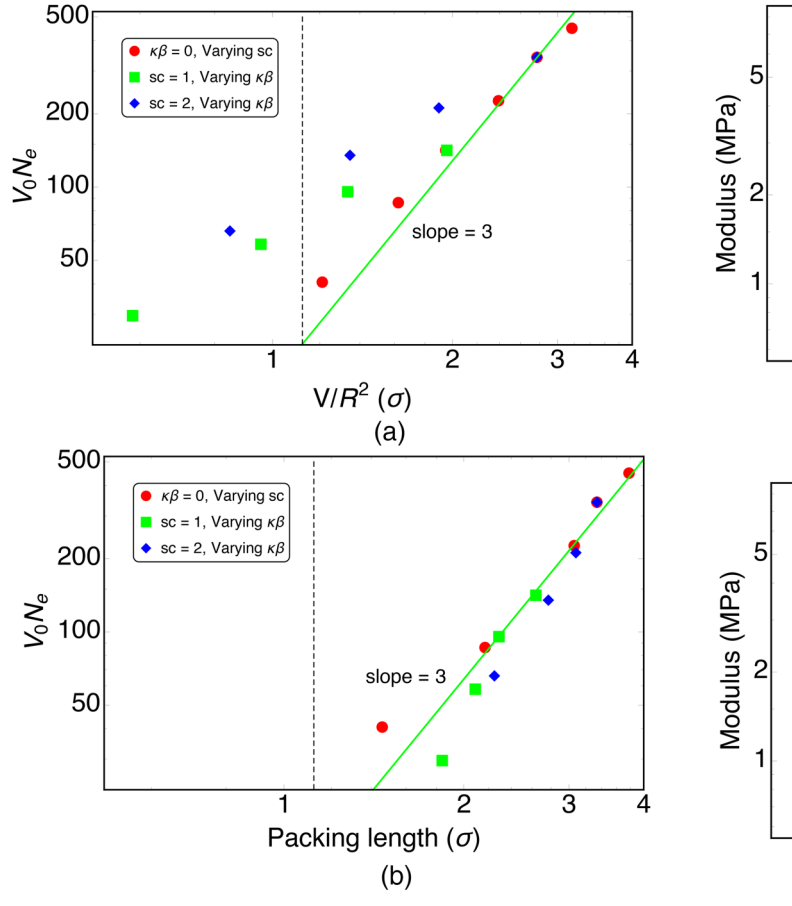


FIG. 7. Entanglement length N_e measured through chain-shrinking technique is plotted against packing length measured in two ways: (a) scaling expression V/R^2 and (b) radial volume fraction. Dashed line represents the bead diameter. Here, V_0 is the number of beads in a monomer, that is, $V_0 = sc + 1$.

we observe the value of p rising. This is not the case when using V/R^2 to measure p. As evident in Fig. 9, V/R^2 reduces to less than the chain diameter for stiff polymers. This expression does not have a lower limit, which is in contradiction with the way p is defined. N_e decreases as the chains are stiffened even in the stiff and semiflexible regimes, as does the expression V/R^2 . This happens due to an increase in the Kuhn length not because of the change in p.

The value of p does depend on the choice of threshold value applied to $F_{other}(r)$. Although a threshold value of 0.5 is intuitive from the way packing length is defined, we have tested thresholds in the range 0.3–0.5. With different thresholds, we obtain different values for packing length; importantly, however, the slopes we observe in Figs. 7(b) and 8(b) remain the same with a different prefactor. (See the supplementary material [19] for plots that illustrate how our results vary with the choice of the threshold value.)

The wiggles in $F_{other}(r)$ shown in Fig. 6 lead to the sensitivity of our method for determining p to the choice of the threshold value. These wiggles ultimately arise from the sharp structures in g(r) evident in Fig. 4. A possible refinement of our approach to reduce this sensitivity would be to convolve g(r) with the form factor of the beads before performing the partial integral of $4\pi r^2 g(r)$ to obtain $F_{other}(r)$.

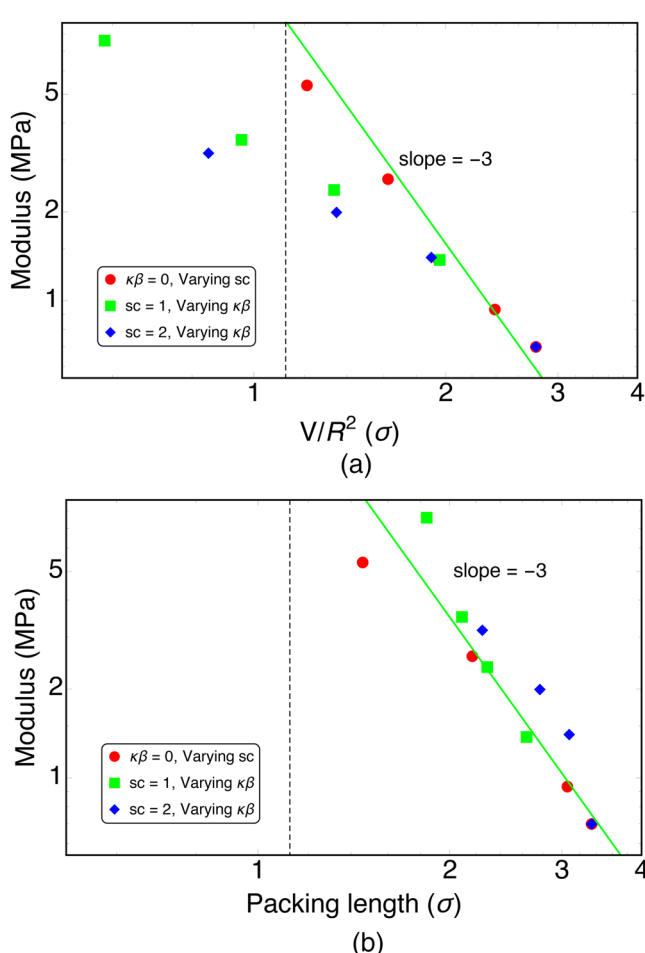


FIG. 8. Entanglement modulus G measured from simulated shearing is plotted against packing length measured in two ways: (a) scaling expression V/R^2 and (b) radial volume fraction. Dashed line represents the bead diameter.

This would in the present case smear g(r) over a distance of 0.1 nm or so, diminishing the peaks in g(r) and hence the wiggles in $F_{other}(r)$.

We recover LN scaling using this improved method of measuring packing length. This refinement was not necessary for the experimental data compiled by Fetters *et al.* [11], for which the scaling expression [Eq. (1)] works well. So why do we have to go to such pains to obtain p? We speculate that Fetters' data comprises polymers with rather flexible backbones and small side groups, similar to the red data points in Fig. 8. Such simulated polymers likewise show agreement with LN scaling when p is estimated by the scaling expression. This approach fails when the simulated polymer backbone becomes stiffer, albeit still in the "flexible" regime due to the bulkiness of the chains. This finding is consistent with our initial assertion that p estimated using Eq. (1) keeps decreasing as the chains stiffen, eventually producing unrealistically small values.

Our new method for obtaining p can be applied to any chain architecture and requires no scaling estimate of chain structural properties such as diameter or stiffness. By measuring $g_{other}(r)$, we include all influence of chain structure, as represented by the conformation and packing of chains in the simulation.

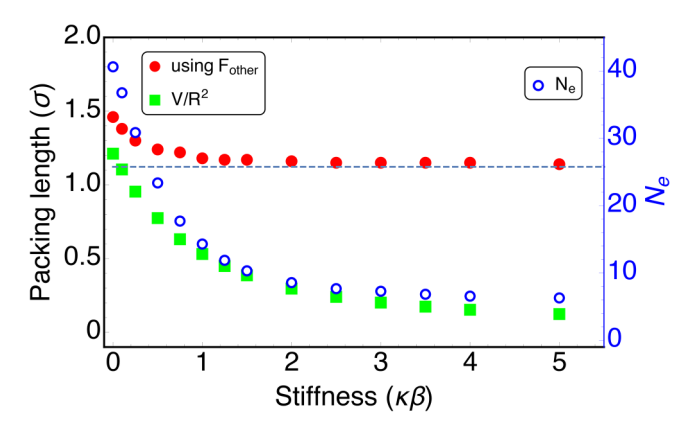


FIG. 9. p is measured in two different ways, the expression V/R^2 and using F_{other} , for stiff and semiflexible polymers with no side chains. N_e is measured using chain-shrinking technique. Dashed line represents the chain diameter $d=2^{1/6}\sigma$.

The intermolecular correlation function $g_{other}(r)$ can, in principle, be obtained from neutron scattering experiments using contrast variation techniques, in which deuterium labeling is used to vary the scattering length density for a dilute mixture of chains in a melt of chemically identical but differently deuterated chains. By varying the contrast between the dilute and background chains, the cross correlation between the dilute chains and background can, in principle, be obtained, the Fourier transform of which is $g_{other}(r)$.

A. Packing length in polymer solutions

Measuring entanglements in solutions of flexible polymers is increasingly challenging as the chains become more dilute. We expect N_e to increase with dilution approximately as $1/\phi$. To measure G or N_e in such solutions, we would need much larger polymers, which would be computationally expensive to investigate because of the larger systems and longer relaxation times required. Here, we investigate the effect of dilution on p, to explore how local correlations affect its value.

We expect the packing length to increase with decreasing concentration of polymers in solution, governed by the solvent quality. When a polymer melt is diluted with a good solvent, chains will swell and exclude other polymers from their correlation blobs. As the nearby fraction of other polymers decreases, the packing length will thus increase. Diluting our melt of purely repulsive chains in vacuum corresponds to the limit of very good solvent.

In contrast, chains swell very little in marginal solvents and theta solutions, so the packing length should increase much less on dilution. We can investigate theta solvents in simulation either by diluting the melt with oligomer chains or by adding attractive interactions to our chains tuned to the theta condition.

In simulations reported below, we explore the impact of polymer concentration and solvent quality on packing length p, for a range of polymer volume fraction ϕ between 0.2 and 1, where $\phi=1$ represents melt density. We varied the concentration of polymer solutions in three different ways. First, we use vacuum as a good solvent for our purely repulsive

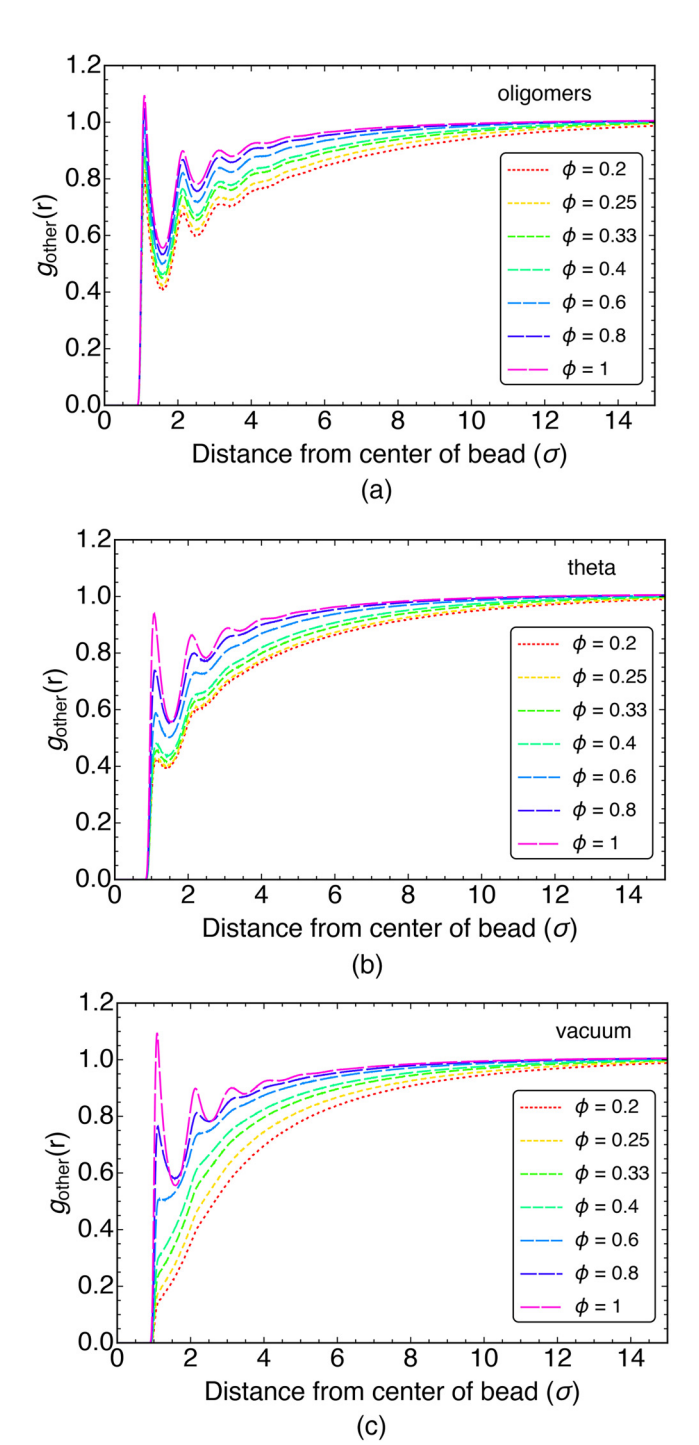


FIG. 10. $g_{other}(r)$ versus r as we vary overall polymer volume fraction using three different types of solvents: (a) oligomer solvent, (b) implicit theta solvent, and (c) vacuum solvent.

chains, by increasing the volume of the simulation box, keeping the number of chains constant. Second, we dilute the polymer system using identical oligomers as a marginal solvent. Third, we vary the polymer concentration at theta condition. We obtain the theta point of polymers using the method described by Graessley *et al.* [20], in which the strength and cutoff distance of the interaction potentials is tuned such that the mean square radius of gyration of dilute polymers is proportional to chain length. Specifically, we increase the Lennard-Jones cutoff length to 2.5σ , so that our

polymer beads are somewhat attractive. Then, we find that for $T=840\,\mathrm{K}$, our chains scale as ideal random walks, indicating we are at the theta temperature. We did not investigate dilution with a monomeric (single bead) solvent. Naïvely, one might expect this to correspond to the best possible solvent conditions; actually, monomeric solvents of identical beads are generally a rather marginal solvent because of depletion attractions induced between bonded chain segments by mobile beads [21].

To simulate these polymer solutions, since we will not attempt to measure N_e or G, we use simple linear bead-spring

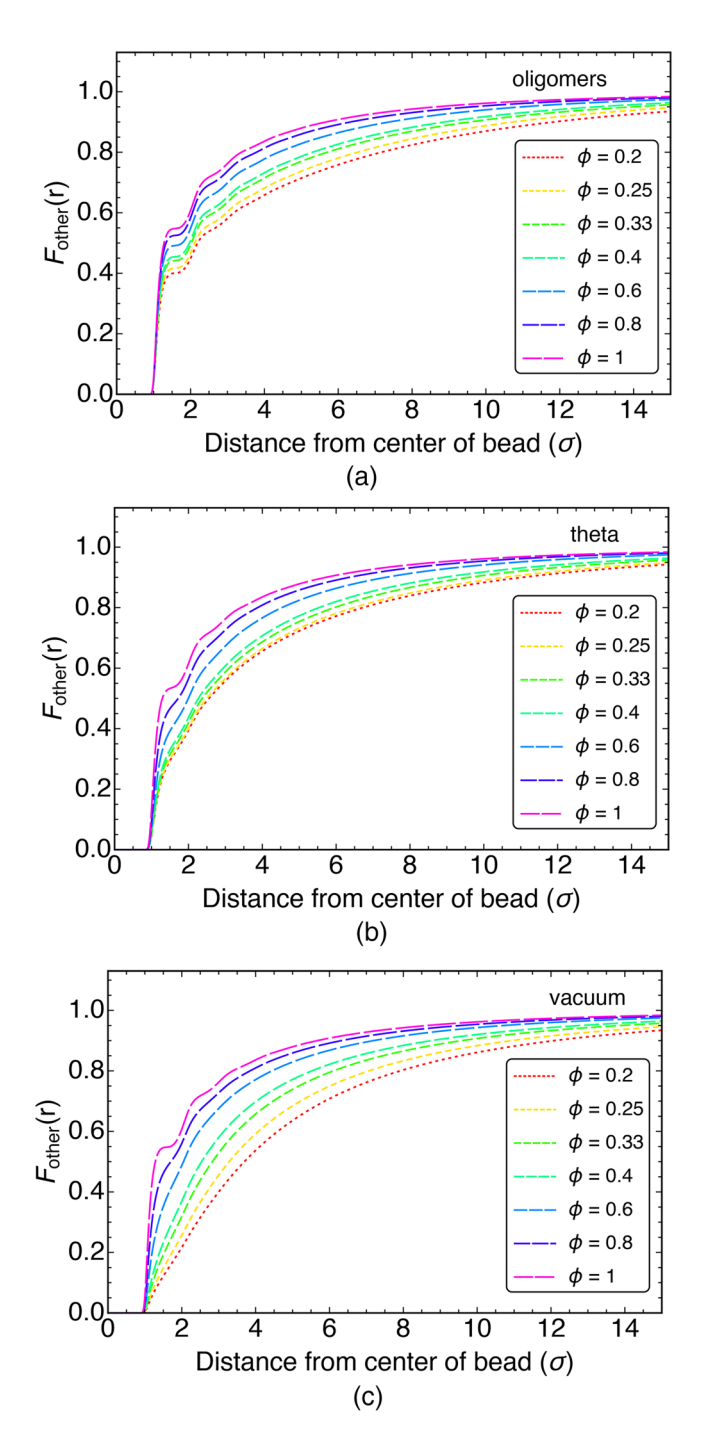


FIG. 11. Radial volume fraction of other polymers $F_{other}(r)$ versus r changes when diluted using: (a) oligomer solvent, (b) implicit theta solvent, and (c) vacuum solvent.

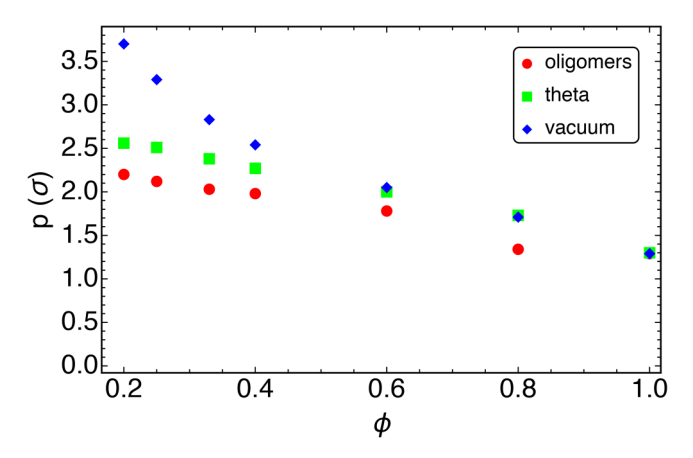


FIG. 12. p versus ϕ shows the increase in packing length as we dilute the polymer solutions using three different types of solvent. Note: data point at $\phi = 0.8$ for oligomers is lower than expected because of the finite size of the beads that causes a small plateau in $F_{other}(r)$.

chains, rather than the ring polymers we used to measure entanglements. For the implicit vacuum and theta solvents, we simulate 100 chains of 200 beads each. For oligomer solutions, we add oligomers of 10 beads each to maintain melt density. We control the concentration by changing the volume and the number of oligomers added to the simulation box.

Polymers are farther apart from each other in solutions than they are in melts. As we dilute the solutions, it is less likely to find other polymers near a given chain. This can be observed from Fig. 10, where the value of $g_{other}(r)$ is smaller near the reference chain for lower concentrations of polymers. As usual for pair correlation functions, $g_{other}(r)$ in Fig. 10 is normalized to approach unity at large distances, for each concentration. Hence, $g_{other}(r)$ can be interpreted as the ratio of the nearby concentration of monomers from other chains, relative to the average value far away.

We define the radial volume fraction of other polymers $F_{other}(r)$ by Eq. (7), just as we did for melts. As we dilute, $F_{other}(r)$ increases more slowly with r (see Fig. 11). As the solvent content increases, chains swell and one must move farther away from the reference polymer for the volume fraction of other polymers to increase to half its average value. Thus, p increases as we dilute the solutions.

Vacuum is an extremely good solvent for purely repulsive chains; hence, the packing length changes more drastically in vacuum than in any other solvent. The changes in packing length in oligomer solvent and at theta condition are very similar, and much less pronounced (as evident in Fig. 12).

IV. CONCLUSION

The packing length is the characteristic distance of the closest approach between polymer backbone segments in a melt. In this work, we presented a new approach to measure the packing length in simulations. This technique is applicable even to polymers for which the chain diameter is difficult to define unambiguously. Unlike the traditional estimate of p as V/R^2 , which can generate unrealistic values less than the chain diameter, our new technique does not produce erroneous values for stiff chains.

We use the radial distribution function $g_{other}(r)$ to obtain the volume fraction of backbone monomers from other nearby chains, as a function of distance from a chosen backbone monomer on a reference chain. From $g_{other}(r)$, we compute the distance at which monomers from other chains start dominating the local density around the reference monomer; we define this distance to be the packing length p.

The entanglement length N_e is measured by chain shrinking and the modulus G is measured by simulated shearing. Using this combined approach, we explore a set of 12 different bead-spring chain melts in which the side group length and backbone stiffness are independently varied, which should result in variations in entanglement. Based on our previous work, all these systems should be in the flexible entanglement regime, for which LN scaling is expected to hold. When p is measured using our technique, both satisfy LN scaling, which also holds for a wide range of polymers as shown by Fetters $et\ al.\ [11]$.

Estimates of the tube diameter based on the packing length as measured here for long entangled linear chains should be valid as well for long-chain branched polymers, such as star polymers, H polymers, and more complex architectures. Indeed, it has been well demonstrated that dynamic rheology of such branched polymers is well described by contemporary tube-based theory, with the same tube diameter used for branched and linear chains [22]. Here, we assume implicity that the long-chain branching is "weak" in that (1) chain segments between branch points are long compared to the entanglement length and (2) branch point functionality is low. Otherwise, chain segments may no longer be essentially Gaussian and entangle locally in the same way as long linear chains. For example, a high-functionality branch point leads to a "corona" region of radially oriented chains to relieve crowding near the branch point.

We showed that $g_{other}(r)$ can be used to measure p in polymer solutions using both implicit and explicit solvents. For purely repulsive chains, vacuum is a very good solvent, in which chains swell markedly. Oligomers serve as a nearly theta solvent, which can also be represented by introducing attractions between monomer beads in vacuum. We find that p always increases with decreasing ϕ , but the magnitude of increase depends markedly on solvent quality.

Measuring p using $g_{other}(r)$ does not depend on any a priori estimates of chain structural parameters and can be applied to any simulated polymer architecture. Structural properties such as chain stiffness, diameter, or monomer chemistry all influence $g_{other}(r)$ and thereby influence the value of the packing length. This allows us to extend this technique to other monomer architectures and atomistic simulations, which will be reported in future publications.

ACKNOWLEDGMENTS

The authors acknowledge financial support from NSF under Award No. DMR-1905632.

REFERENCES

 Rubinstein, M., and R. H. Colby, *Polymer Physics* (Oxford University, New York, 2003), Vol. 23.

- [2] Edwards, S., "The statistical mechanics of polymerized material," Proc. Phys. Soc. 92, 9–16 (1967).
- [3] de Gennes, P.-G., "Reptation of a polymer chain in the presence of fixed obstacles," J. Chem. Phys. 55, 572–579 (1971).
- [4] Doi, M., and S. F. Edwards, *The Theory of Polymer Dynamics* (Oxford University, New York, 1988), Vol. 73.
- [5] Milner, S. T., "Unified entanglement scaling for flexible, semiflexible, and stiff polymer melts and solutions," Macromolecules 53, 1314–1325 (2020).
- [6] Witten, T. A., S. T. Milner, and Z. G. Wang, Theory of stress distribution in block copolymer microdomains, in *Contemporary Topics in Polymer Science, Vol. 6, Multiphase Macromolecular Systems* (Plenum Press, New York, 1989), pp. 655–663.
- [7] Fetters, L. J., D. J. Lohse, S. T. Milner, and W. W. Graessley, "Packing length influence in linear polymer melts on the entanglement, critical, and reptation molecular weights," Macromolecules 32, 6847–6851 (1999).
- [8] Fetters, L., D. Lohse, and R. Colby, "Chain dimensions and entanglement spacings," in *Physical Properties of Polymers Handbook* (Springer, Berlin, 2007), pp. 447–454.
- [9] Lin, Y., "Number of entanglement strands per cubed tube diameter, a fundamental aspect of topological universality in polymer viscoelasticity," Macromolecules 20, 3080–3083 (1987).
- [10] Kavassalis, T. A., and J. Noolandi, "New view of entanglements in dense polymer systems," Phys. Rev. Lett. 59, 2674–2677 (1987).
- [11] Fetters, L. J., D. J. Lohse, D. Richter, T. A. Witten, and A. Zirkel, "Connection between polymer molecular weight, density, chain dimensions, and melt viscoelastic properties," Macromolecules 27, 4639–4647 (1994).
- [12] Uchida, N., G. S. Grest, and R. Everaers, "Viscoelasticity and primitive path analysis of entangled polymer liquids: From F-actin to polyethylene," J. Chem. Phys. 128, 044902 (2008).
- [13] Bobbili, S. V., and S. T. Milner, "Simulation study of entanglement in semiflexible polymer melts and solutions," Macromolecules 53, 3861–3872 (2020).
- [14] Qin, J., and S. T. Milner, "Tube dynamics works for randomly entangled rings," Phys. Rev. Lett. 116, 068307 (2016).
- [15] Everaers, R., S. K. Sukumaran, G. S. Grest, C. Svaneborg, A. Sivasubramanian, and K. Kremer, "Rheology and microscopic topology of entangled polymeric liquids," Science 303, 823–826 (2004).
- [16] Sukumaran, S. K., G. S. Grest, K. Kremer, and R. Everaers, "Identifying the primitive path mesh in entangled polymer liquids," J. Polym. Sci., Part B: Polym. Phys. 43, 917–933 (2005).
- [17] Kröger, M., "Shortest multiple disconnected path for the analysis of entanglements in two- and three-dimensional polymeric systems," Comput. Phys. Commun. 168, 209–232 (2005).
- [18] Shanbhag, S., and M. Kröger, "Primitive path networks generated by annealing and geometrical methods: Insights into differences," <u>Macromolecules</u> 40, 2897–2903 (2007).
- [19] See the supplementary material at https://doi.org/10.1122/8.0000305 for discussion and graphs illustrating the extent to which our results for packing length p depend on the cutoff value chosen for the fraction $F_{other}(r)$ at r = p.
- [20] Graessley, W. W., R. C. Hayward, and G. S. Grest, "Excluded-volume effects in polymer solutions. 2. Comparison of experimental results with numerical simulation data," Macromolecules 32, 3510–3517 (1999).
- [21] Milner, S. T., M.-D. Lacasse, and W. W. Graessley, "Why χ is seldom zero for polymer- solvent mixtures," Macromolecules 42, 876–886 (2009).
- [22] McLeish, T., and S. T. Milner, "Entangled dynamics and melt flow of branched polymers," Branched Polymers II 143, 195–256 (1999).